remote sensing

MDPI

Communication

Casual Rerouting of AERONET Sun/Sky Photometers: Toward a New Network of Ground Measurements Dedicated to the Monitoring of Surface Properties?

Dominique Carrer [1,*], Catherine Meurey [1], Olivier Hagolle [2], Guillaume Bigeard [1], Alexandre Paci [1], Jean-Marie Donier [1], Gilles Bergametti [3], Thierry Bergot [1], Jean-Christophe Calvet [1], Philippe Goloub [4], Stéphane Victori [5] and Zhuosen Wang [6,7]

[1] Centre National de Recherches Météorologiques (CNRM), Université de Toulouse, Météo France, CNRS, 42 Avenue Gaspard Coriolis, 31057 Toulouse, France; catherine.meurey@meteo.fr (C.M.); guillaume.bigeard@meteo.fr (G.B.); alexandre.paci@meteo.fr (A.P.); jean-marie.donier@meteo.fr (J.-M.D.); thierry.bergot@meteo.fr (T.B.); jean-christophe.calvet@meteo.fr (J.-C.C.)
[2] CESBIO, UMR 5126. 18 Avenue Edouard Belin, bpi 2801, CEDEX 9, 31401 Toulouse, France; olivier.hagolle@cnes.fr
[3] Laboratoire Interuniversitaire des Systèmes Atmosphériques (LISA), UMR CNRS 7583, Université de Paris and Université Paris Est, IPSL, 94010 Creteil, France; Gilles.Bergametti@lisa.u-pec.fr
[4] LOA, Laboratoire d'Optique Atmosphérique-UMR 8518, 59000 Lille, France; philippe.goloub@univ-lille.fr
[5] CIMEL ELECTRONIQUE, Laboratoire Charles Fabry, 75001 Paris, France; s-victori@cimel.fr
[6] NASA, Goddard Space Flight Center (GSFC), Greenbelt, MD 20771, USA; zhuosen.wang@nasa.gov
[7] Earth System Science Interdisciplinary Center, University of Maryland, College Park, MD 20742, USA
* Correspondence: dominique.carrer@meteo.fr

Citation: Carrer, D.; Meurey, C.; Hagolle, O.; Bigeard, G.; Paci, A.; Donier, J.-M.; Bergametti, G.; Bergot, T.; Calvet, J.-C.; Goloub, P.; et al. Casual Rerouting of AERONET Sun/Sky Photometers: Toward a New Network of Ground Measurements Dedicated to the Monitoring of Surface Properties? *Remote Sens.* **2021**, *13*, 3072. https://doi.org/10.3390/rs13163072

Academic Editor: Pradeep Wagle

Received: 24 June 2021
Accepted: 3 August 2021
Published: 4 August 2021

Abstract: This paper presents an innovative method for observing vegetation health at a very high spatial resolution (~5 × 5 cm) and low cost by upgrading an existing Aerosol RObotic NETwork (AERONET) ground station dedicated to the observation of aerosols in the atmosphere. This study evaluates the capability of a sun/sky photometer to perform additional surface reflectance observations. The ground station of Toulouse, France, which belongs to the AERONET sun/sky photometer network, is used for this feasibility study. The experiment was conducted for a 5-year period (between 2016 and 2020). The sun/sky photometer was mounted on a metallic structure at a height of 2.5 m, and the acquisition software was adapted to add a periodical (every hour) ground-observation scenario with the sun/sky photometer observing the surface instead of being inactive. Evaluation is performed by using a classical metric characterizing the vegetation health: the normalized difference vegetation index (NDVI), using as reference the satellite NDVI derived from a Sentinel-2 (S2) sensor at 10 × 10 m resolution. Comparison for the 5-year period showed good agreement between the S2 and sun/sky photometer NDVIs (i.e., bias = 0.004, RMSD = 0.082, and R = 0.882 for a mean value of S2A NDVI around 0.6). Discrepancies could have been due to spatial-representativeness issues (of the ground measurement compared to S2), the differences between spectral bands, and the quality of the atmospheric correction applied on S2 data (accuracy of the sun/sky photometer instrument was better than 0.1%). However, the accuracy of the atmospheric correction applied on S2 data in this station appeared to be of good quality, and no dependence on the presence of aerosols was observed. This first analysis of the potential of the CIMEL CE318 sun/sky photometer to monitor the surface is encouraging. Further analyses need to be carried out to estimate the potential in different AERONET stations. The occasional rerouting of AERONET stations could lead to a complementary network of surface reflectance observations. This would require an update of the software, and eventual adaptations of the measurement platforms to the station environments. The additional cost, based on the existing AERONET network, would be quite limited. These new surface measurements would be interesting for measurements of vegetation health (monitoring of NDVI, and also of other vegetation indices such as the leaf area and chlorophyll indices), for validation and calibration exercise purposes, and possibly to refine various scientific algorithms (i.e., algorithms dedicated to cloud detection or the AERONET aerosol retrieval algorithm itself). CIMEL is ready to include the ground scenario used in this study in all new sun/sky photometers.

Keywords: AERONET; vegetation; satellite; Sentinel-2; validation; photometer; surface; aerosol

1. Introduction

The physical and optical characteristics of atmospheric particles can be determined over selected regions using the Aerosol Robotic Network (AERONET), which encompasses hundreds of stations around the world, equipped with sun/sky scanning spectral photometers [1]. Conceived in the early 1990s, AERONET is a network of autonomously operated CIMEL Electronique sun/sky photometers, used to measure sun and moon collimated direct-beam irradiance and directional sky radiance. This network provides quality-assured, column-integrated aerosol microphysical and radiative properties and aerosol optical depth (AOD). The AERONET network has operated for more than 25 years thanks to the investments and efforts of NASA (Goddard Space Flight Center, GSFC, Greenbelt, MD, USA) [1], the University of Lille (PHOtométrie pour le Traitement Opérationnel de Normalisation Satellitaire—PHOTONS) [2], with the support of Centre National d'Etudes Spatiales (CNES) and Centre National de la Recherche Scientifique (CNRS), University of Valladolid (Red Ibérica de medida Fotométrica de Aerosoles—RIMA) [3], other subnetworks (e.g., [4–7]), collaborators at agencies, institutes, universities, and individual scientists globally.

AERONET's primary objective is to provide an aerosol database for the validation of Earth Observing System (EOS) satellite retrievals of AOD and atmospheric correction. AERONET data were gradually used to open new perspectives in the domain. The first study for correcting the aerosol effects on remote sensing using AERONET was conducted in 1996 by Kaufman and Tanré [8]. In addition to columnar direct Sun AOD, sky radiance was initially used to infer aerosol characteristics from Nakajima et al. in 1996 [9], followed by Schafer in 2014 [10], Andrews in 2017 [11], and Sinyuk et al. in 2020 [12]. Later, Dubovik and King [13] obtained products such as aerosol volume-size distribution, complex index of refraction, single scattering albedo, and phase functions. However, these studies poorly investigated the interest of pointing a sun/sky photometer in a downward direction to the surface. The RObotic Station for Atmosphere and Surface characterization (ROSAS) [14] and HYPERNETS [15] initiatives intend to set up automatic photometric measurements to characterize surface-directional reflectance properties (and the optical properties of the atmosphere for ROSAS). However, there are a limited number of stations: 3 stations in the south of France and Namibia for ROSAS, and fewer than 20 for HYPERNETS. Also, the following question may be raised: What can be expected from the extensive AERONET network for the monitoring of surface properties?

The objective of this study is to evaluate the capability of a sun/sky photometer from the AERONET network to observe the surface, in addition to the atmosphere. Section 2 describes the materials and methods, and the experiment protocol. Section 3 shows the results through a comparison with independent satellite-derided products used as reference. The limitations and perspectives of the method are discussed in Section 4, before concluding in Section 5.

2. Materials and Methods

2.1. Photometer Measurements

2.1.1. Default Configuration

The experimental in situ station is located in Toulouse, Southwest France on the Meteopole instrument site (http://www.umr-cnrm.fr/spip.php?rubrique279, last consulted on 4 August 2021). It is a grassland field of about 10 hectares, spatially homogeneous and located close to the research laboratory building on Météo France site (43.572°N; 1.374°E; 160 m above sea level; Figure 1). Except for lawn mowing, which is performed when the vegetation becomes very high (1 to 2 times per year, mainly in summer), there is no management of this area, and only a few persons access it for the maintenance of other instruments (e.g., for soil temperature and humidity, wind, air temperature, or radiative fluxes).

Figure 1. Location of sun/sky photometer on instrumented Meteopole Toulouse site, France (red dot, courtesy of Google Earth).

A CIMEL CE318 sun/sky photometer belonging to the AERONET network and operating in 9 bands ranging from 340 to 1640 nm (340, 380, 440, 500, 675, 870, 937, 1020, and 1640 nm) was installed in 2013. In the frame of the services of PHOTONS, the instrument operated at this site was replaced by another, having the same characteristics each time maintenance and calibration issues were needed. Thus, five sun/sky photometers were successively installed from 2016 to 2020 (AERONET identity numbers 715, 842, 714, 347, and 141). Several hundreds of sun/sky photometers belonging to the AERONET network (Figure 2) are continuously and, in near real-time, observing the atmosphere around the world. More information about the AOD measured from the Meteopole Toulouse station (Météo France, Paris, France), called 'Toulouse_MF', is available on https://aeronet.gsfc.nasa.gov/cgibin/data_display_aod_v3?site=Toulouse_MF&nachal=2&level=3&place_code=10 (last consulted on 4 August 2021).

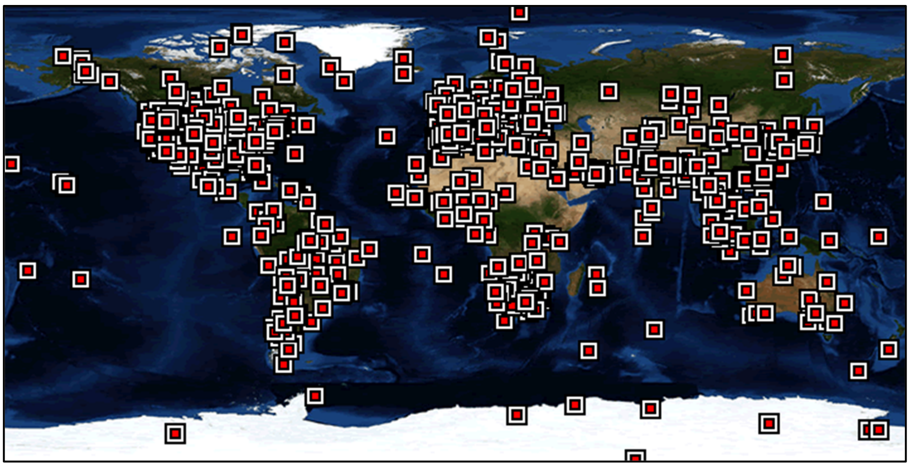

Figure 2. Location of sun/sky photometers belonging to the AERONET network (red dots), courtesy of https://aeronet.gsfc.nasa.gov (last consulted on 4 August 2021).

2.1.2. Hybrid Configuration

In 2016, the AERONET sun/sky photometer was mounted on a metallic structure at a height of 2.5 m (Figure 3). The acquisition software was adapted to add a new and brief scenario (a few minutes) to perform surface spectral radiance measurements every hour when the photometer aimed towards the surface. Figure 3 shows the sun/sky photometer and its rotation from the sun direction to the surface direction with an inclination of 30 degrees. Considering the focal length of the sun/sky photometer and its distance from the ground, the footprint of the sun/sky photometer measurement in the surface direction was 5.7 × 5.7 cm. Five years of such surface measurements (2016–2020) were used in this study.

(**a**)

(**b**) (**c**) (**d**)

Figure 3. Toulouse sun/sky photometer: (**a**) pointing towards the sun; (**b**,**c**) rotating toward the surface; and (**d**) stand-by condition between two measurements.

2.2. *Sentinel-2 Data*

The Copernicus Sentinel-2 (S2) mission comprises two twin polar-orbiting satellites, Sentinel-2A (S2A) and Sentinel 2B (S2B), placed in the same sun-synchronous orbit, phased at 180 degrees to each other, and launched on 23 June 2016 and 7 March 2017, respectively. Sentinel-2 has a wide swath width of 290 km and a revisit time of around 10 days at the equator with one satellite (around 5 days with two satellites). It provides geographical information used for the monitoring of land cover, vegetation state, water cycle, marine ecosystems, natural disasters, etc. The S2 satellites carry a multispectral instrument (MSI) that measures reflected solar spectral radiance in 13 spectral bands, ranging from the visible to the shortwave infrared bands at high-to-moderate spatial resolution (i.e., 10 to 60 m) [14,16]. Spectral Sentinel-2 radiance at the top of atmosphere was corrected for atmospheric effects, and clouds were filtered out by the CNES agency using MAJA software [17]. Level 2 spectral S2 radiance data at the top of canopy level were downloaded from the Theia land data center (https://theia.cnes.fr/, last consulted on 4 August 2021). They comprise two bands (664 and 865 nm) corresponding to chlorophyll absorption (670 nm) and infrared edge (870 nm), used for the computation of the normalized difference vegetation index (NDVI).

2.3. Experiment Setup

The objective of this study was to evaluate the potential of AERONET sun/sky photometers for the observation of the surface properties. S2 radiances at the top of canopy level, after atmospheric correction (see Section 2.2) and after filtering residual cloud contaminations, were compared to the sun/sky photometer measurements at 5 × 5 cm pointing to the surface direction (see Section 2.1.2).

Accurate direct comparisons between sun/sky photometer and S2 observations need to account for the difference in the type of measurements. Indeed, S2 data from the Theia land data center are in reflectance units, while sun/sky photometer data were in digital units. Light that is collimated, not scattered, or absorbed by the atmosphere, and bounces back by the surface illuminates the photodiode detector of the sun/sky photometer. This light energy is converted into a digital signal, and its magnitude depends on the size of the detector, its geometric orientation with regard to the sun, the spectral sensitivity of the sensor, etc. In order to circumvent the unit differences between satellite and sun/sky photometer measurements, the comparison was performed on the basis of a dimensionless metric, the classical relative ratio normalized difference vegetation index (NDVI):

$$\text{NDVI} = \frac{R(\lambda_2)\ -\ R(\lambda_2)}{R(\lambda_1) + R(\lambda_2)} \tag{1}$$

where R is the radiance measured at = 675 nm (664 nm at 10 × 10 m resolution) and =870 nm (865 nm at 20 × 20 m resolution) for the sun/sky photometer (S2 instrument). The NDVI is one of the most common indices widely applied for monitoring vegetation dynamics at regional and global scales [18,19]. This index was introduced by Tucker in 1979 [20] and varies between −1 and 1. Values greater than 0.3 indicate the presence of vegetation cover.

First, qualitative analysis was performed by comparing the temporal evolution of the sun/sky photometer-derived NDVI and S2-derived NDVI. Second, a scatter plot between both NDVIs and statistical scores (bias, root-mean-square deviation (RMSD), and correlation score (R)) were used for quantitative evaluation. Third, trends were analyzed by comparing the differences between both NDVIs and the AOD at 675 nm.

3. Results

Figure 4 reports the time series of sun/sky photometer-derived NDVI and S2-derived NDVI. Sun/sky photometer-derived NDVIs were daily averaged values (magnitudes of the diurnal variation of the index were small). S2-derived NDVIs were calculated by using data from orbit number 51 at 10:58 UTC.

In the Toulouse station, the NDVI decreased from 0.8 (wet conditions) in spring to a minimal value of approximately 0.3 at the end of the summer period (dry conditions). Quite good agreement existed between both NDVIs, with the same timings and magnitudes of the temporal changes along seasonal cycles. The performance of all sun/sky photometers was comparable by considering S2 as a reference. S2A and S2B allow for observing the surface every 18 days on average at this station (total number of clear-sky observations was 99 over the 5-year period). By comparison, the sun/sky photometer can make observations of the surface several times per day.

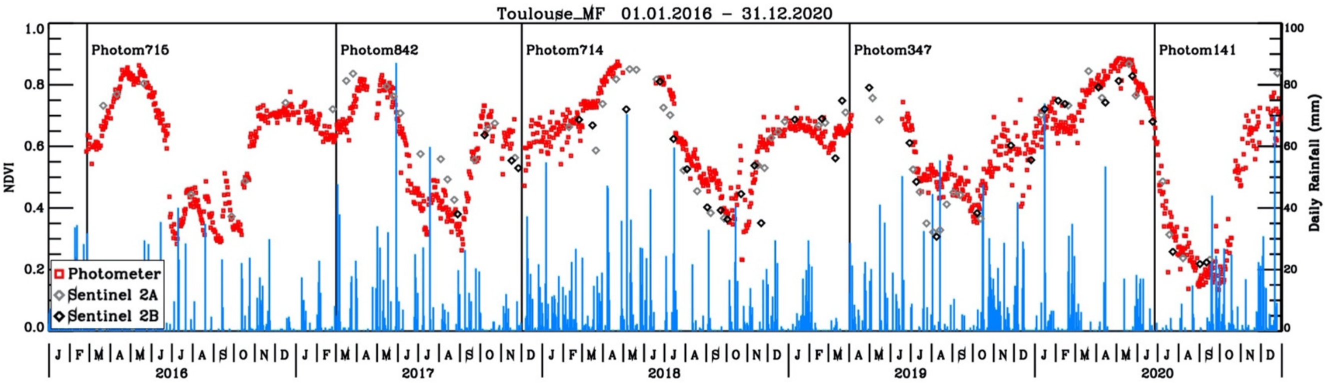

Figure 4. Time series from 2016 to 2020 of sun/sky photometer-derived NDVI (in red) and S2-derived NDVI in Toulouse station, France (in gray for S2A L2A, and in black for S2B L2A). Vertical blue lines show the daily rainfalls (in mm).

Figure 5 shows the scatter plot between sun/sky photometer-derived NDVI and S2-derived NDVI. Bias and RMSD on a daily basis between both NDVIs were small and correlation important: bias = 0.004 (0.024), RMSD = 0.082 (0.081), and R = 0.882 (0.899) by using S2A NDVI as reference (S2B, respectively). The mean annual value of NDVI in the Toulouse_MF station was around 0.6. It is difficult to state if these small discrepancies between S2- and sun/sky photometer NDVIs were due to rainstorms and water-soaked soils (see rainfall in blue, Figure 4). However, several causes may explain these differences: spectral response differences between S2 and sun/sky photometer bands, spatial-representativeness issues, and the quality of the atmospheric correction applied on S2 data (accuracy of the sun/sky photometer instrument was less than 0.1%). Figure 6 investigates the impact of the accuracy of the atmospheric correction by comparing the absolute bias between both NDVIs and the daily AOD at 675 nm observed by AERONET. No specific trend was observed, which tends to confirm the quality of atmospheric correction performed on S2 data.

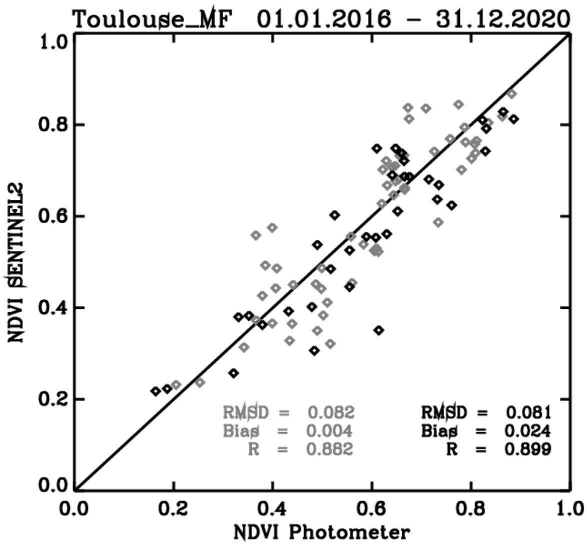

Figure 5. Scatter plot between S2-derived NDVI and sun/sky photometer-derived NDVI in Toulouse station, France (in gray for S2A L2A, and in black for S2B L2A).

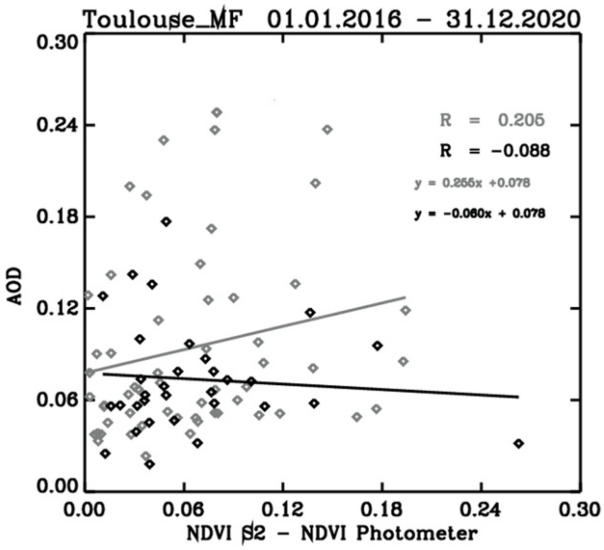

Figure 6. Scatter plot between daily AOD at 675 nm and the absolute difference between S2-derived NDVI and sun/sky photometer-derived NDVI in Toulouse station, France (in gray for S2A L2A, and in black for S2B L2A).

4. Discussion

This first analysis of the potential of the CIMEL CE318 instrument operated in AERONET for the monitoring of surface properties is encouraging.

The setup of a complementary network of surface reflectance observations based on AERONET would require an update of the software to make measurements pointing towards the surface, and eventual adaptations of the measurement platforms to the station environments. The additional cost, based on this existing AERONET network, would be quite low. The update of the acquisition software could be conducted during the annual calibration or maintenance phase of the instrument (possible adjustment of instrument setup may also be considered). CIMEL is proposing to include the upgrade used in this study, called ground scenario, in all new sun/sky photometers. No degradation would affect the existing AERONET network (quality and frequency of aerosol-load observations as the sun/sky photometers would be unchanged). However, people in charge of AERONET stations who are interested in this ground scenario may have to be invited to adopt best practices (which would need to be defined) for the installation of the sun/sky photometers pointing towards the surface. If a decision is made to deploy this subnetwork of AERONET, the authors of this study would like to call it AEROnet Network Used for Surface (AERONUS).

However, one of the main limitations of the system is the small spatial representativeness of the measurement. A sun/sky photometer at a height of 2.5 m observes only a surface footprint of approximately 5 × 5 cm. An instrument installed at a higher height would only allow for a small increase in the footprint of the measurement. An elegant solution for this problem of footprint would be to adapt the acquisition software to allow for observations at different viewing angles over a period of a few seconds. This could allow evaluation of the heterogeneity of the vegetation cover and health up to an area of about 60 × 60 m for an inclination of 85 degrees and an instrument at 2.5 m height.

This is a feasibility study and thus used the NDVI metric by only exploiting two spectral bands. Lange et al. [21] showed that ground measurements of NDVI from a multispectral instrument and satellite NDVI correlate well (0.72 < r2 < 0.97) over temperate deciduous forest. This study shows correlation between multispectral and satellite NDVIs of about 0.9. As AERONET sun/sky photometers usually have 9 spectral bands, they could offer additional perspectives for the monitoring of different vegetation-health indices (such as the leaf area, chlorophyll content, and pigment indices). Table 1 gives a nonexhaustive list of indices that could be derived from these 9 spectral bands.

Table 1. Examples of indices (nonexhaustive) that can be derived from spectral CIMEL sun/sky photometer bands (detailed information about their calculations available in [22–24]).

Index	CIMEL Sun/Sky Photometer Spectral Bands (in nm)								
	340	**380**	**440**	**500**	**675**	**870**	**937**	**1020**	**1640**
CI2 (carotenoid index 2)				x	x				
EVI (enhanced vegetation index)			x		x	x			
EVI2 (enhanced vegetation index 2)					x	x			
LWVI-1 (normalized difference leaf water)							x	x	
MSAVI2 (modified soil-adjusted vegetation index)					x	x			
NBR (normalized burn ratio)						x			x
NDVI (normalized difference vegetation index)					x	x			
NPCI (normalized pigment chlorophyll index)			x		x				
SAVI (soil-adjusted vegetation index)					x	x			
SIWSI (vegetation water content)						x			x
SLAVI (specific-leaf-area vegetation index)					x	x			x
SR (simple ratio)					x	x			
SR3 (simple ratio 3)			x		x				

5. Summary

This study demonstrated the good performance of AERONET sun/sky photometers to perform additional observations of the surface reflectance. The NDVI metric was chosen for evaluation due to its wide use for the monitoring of vegetation health by the scientific community since the 1980s. As the NDVI metric is also the relative difference between two spectral bands, it allowed us to make direct comparisons between S2 and sun/sky photometer measurements without considering the unit differences. The comparisons showed good agreement between both NDVIs, with the same timings and magnitudes of the temporal changes along seasonal cycles. Bias and RMSD between S2A- and sun/sky photometer-derived NDVIs were small, 0.004 and 0.082, respectively (for a mean value of NDVI around 0.6) for the 5-year period of analysis (2016–2020). Correlation was very high, close to 0.9. The same performance was found between S2B-derived and sun/sky photometer-derived NDVIs.

These results illustrate the important capability of AERONET sun/sky photometers for monitoring surface properties (especially by using different combinations of the 9 spectral bands usually available today). These new surface measurements are also interesting for validation and calibration purposes, may contribute to refining various scientific algorithms (e.g., algorithms dedicated to cloud detection, or the AERONET aerosol retrieval algorithm itself), and may find applications in other domains (e.g., detection of frozen periods and impact on vegetation). This study may also motivate people in charge of other AERONET stations to operate this casual rerouting of AERONET sun/sky photometers, and to develop a complementary network of ground measurements dedicated to the monitoring of surface properties.

Author Contributions: Conceptualization, D.C. and C.M.; software, J.-M.D., P.G. and A.P.; formal analysis, D.C., C.M., G.B. (Guillaume Bigeard), G.B. (Gilles Bergametti), T.B., J.-C.C., O.H., P.G., A.P., S.V., and Z.W. All authors have read and agreed to the published version of the manuscript.

Funding: The authors wish to acknowledge the members of the AERONET teams, and Météo France.

Acknowledgments: We thank AERONET for access to the data. We thank the CNRM/GMEI group (especially GMEI/TRAMM and 4M) for the maintenance of the Meteopole Toulouse instrumented site. We thank the CNRM/GMEI/LISA and LOA teams (especially L. Blarel) for the maintenance of the sun/sky photometer used in this study. We also thank T. Douffet and S. Rieublanc for the adaptation of the structure supporting the instrument in order to allow for it to aim at the surface.

Conflicts of Interest: The authors declare no conflict of interest.

References

1. Holben, B.; Eck, T.; Slutsker, I.; Tanré, D.; Buis, J.; Setzer, A.; Vermote, E.; Reagan, J.; Kaufman, Y.; Nakajima, T.; et al. AERONET: A federated instrument network and data archive for aerosol characterization. *Remote Sens. Environ.* **1998**, *66*, 1–16. [CrossRef]
2. Goloub, P.; Li, Z.; Dubovik, O.; Blarel, L.; Podvin, T.; Jankowiak, I.; Lecoq, R.; Deroo, C.; Chatenet, B.; Morel, J.P.; et al. PHOTONS/AERONET Sun-photometer network overview: Description, activities, results. *Proc. SPIE* **2008**, *6936*, 69360V. [CrossRef]
3. Toledano, C.; González, R.; Fuertes, D.; Cuevas, E.; Eck, T.F.; Kazadzis, S.; Kouremeti, N.; Gröbner, J.; Goloub, P.; Blarel, L.; et al. Assessment of Sun photometer Langley calibration at the high-elevation sites Mauna Loa and Izaña. *Atmos. Chem. Phys.* **2018**, *18*, 14555–14567. [CrossRef]
4. Bokoye, A.I.; Royer, A.; O'Neill, N.T.; Cliche, P.; Fedosejevs, G.; Teillet, P.M.; McArthur, L.J.B. Characterization of atmospheric aerosols across Canada from a ground-based Sun-photometer network: AEROCAN. *Atmos. Ocean* **2001**, *39*, 429–456. [CrossRef]
5. Mitchell, R.M.; Forgan, B.W.; Campbell, S.K. The Climatology of Australian Aerosol. *Atmos. Chem. Phys.* **2017**, *17*, 5131–5154. [CrossRef]
6. Sakerin, S.M.; Kabanov, D.M.; Panchenko, M.V.; Pol'kin, V.V.; Holben, B.N.; Smirnov, A.V.; Beresnev, S.A.; Gorda, S.Y.; Kornienko, G.I.; Nikolashkin, S.V.; et al. Monitoring of atmospheric aerosol in the Asian part of Russia in 2004 within the framework of AEROSIBNET program. *Atmos. Ocean. Opt.* **2005**, *18*, 871–878.
7. Che, H.; Zhang, X.-Y.; Xia, X.; Goloub, P.; Holben, B.; Zhao, H.; Wang, Y.; Zhang, X.-C.; Wang, H.; Blarel, L.; et al. Ground-based aerosol climatology of China: Aerosol optical depths from the China Aerosol Remote Sensing Network (CARSNET) 2002–2013. *Atmos. Chem. Phys.* **2015**, *15*, 7619–7652. [CrossRef]
8. Kaufman, Y.J.; Tanré, D. Strategy for direct and indirect methods for correcting the aerosol effect on remote sensing: From AVHRR to EOS-MODIS. *Remote Sens. Environ.* **1996**, *55*, 65–79. [CrossRef]
9. Nakajima, T.; Tonna, G.; Rao, R.; Boi, P.; Kaufman, Y.; Holben, B. Use of sky brightness measurements from ground for remote sensing of particulate polydispersions. *Appl. Opt.* **1996**, *35*, 2672–2686. [CrossRef] [PubMed]
10. Schafer, J.S.; Eck, T.F.; Holben, B.N.; Thornhill, K.L.; Anderson, B.E.; Sinyuk, A.; Giles, D.M.; Winstead, E.L.; Ziemba, L.D.; Beyersdorf, A.J.; et al. Intercomparison of aerosol single-scattering albedo derived from AERONET surface radiometers and LARGE in situ aircraft profiles during the 2011 DRAGON-MD and DISCOVER-AQ experiments. *J. Geophys. Res. Atmos.* **2014**, *119*, 7439–7452. [CrossRef]
11. Andrews, E.; Ogren, J.A.; Kinne, S.; Samset, B. Comparison of AOD, AAOD and column single scattering albedo from AERONET retrievals and in situ profiling measurements. *Atmos. Chem. Phys.* **2017**, *17*, 6041–6072. [CrossRef]
12. Sinyuk, A.; Holben, B.N.; Eck, T.F.; Giles, D.M.; Slutsker, I.; Korkin, S.; Schafer, J.S.; Smirnov, A.; Soroki, M.; Lyapustin, A. The AERONET Version 3 aerosol retrieval algorithm, associated uncertainties and comparisons to Version 2. *Atmos. Meas. Tech.* **2020**, *13*, 3375–3411. [CrossRef]
13. Dubovik, O.; King, M.D. A flexible inversion algorithm for retrieval of aerosol optical properties from Sun and sky radiance measurements. *J. Geophys. Res.* **2000**, *105*, 20673–20696. [CrossRef]
14. Meygret, A.; Santer, R.P.; Berthelot, B. ROSAS: A robotic station for atmosphere and surface characterization dedicated to on-orbit calibration. *Proc. SPIE* **2011**, *8153*, 815311. [CrossRef]
15. Goyens, C.; Ruddick, K.; Kuusk, J. Spectral Requirements for the Development of a New Hyperspectral Radiometer Integrated in Automated Networks—The Hypernets Sensor. In Proceedings of the 2018 9th Workshop on Hyperspectral Image and Signal Processing: Evolution in Remote Sensing (WHISPERS), Amsterdam, The Netherlands, 23–26 September 2018; pp. 1–5. [CrossRef]
16. Drusch, M.; del Bello, U.; Carlier, S.; Colin, O.; Fernandez, V.; Gascon, F.; Hoersch, B.; Isola, C.; Laberinti, P.; Martimort, P. Sentinel-2: ESA's optical high-resolution mission for GMES operational services. *Remote Sens. Environ.* **2012**, *120*, 25–36. [CrossRef]
17. Hagolle, O.; Colin, J.; Kettig, P.; d'Angelo, P.; Auer, S.; Doxani, G.; Coustance, C.; Desjardins, C. Sentinel-2 surface reflectance products generated by THEIA and DLR: Methods, validation and applications. *ISPRS Ann. Photogramm. Remote Sens. Spat. Inf. Sci.* **2021**, *1*, 9–15. [CrossRef]
18. Vrieling, A.; De Leeuw, J.; Said, M.Y. Length of Growing Period over Africa: Variability and Trends from 30 Years of NDVI Time Series. *Remote Sens.* **2013**, *5*, 982. [CrossRef]
19. Zhu, Z.; Bi, J.; Pan, Y.; Ganguly, S.; Anav, A.; Xu, L.; Samanta, A.; Piao, S.; Nemani, R.R.; Myneni, R.B. Global Data Sets of Vegetation Leaf Area Index (LAI)3g and Fraction of Photosynthetically Active Radiation (FPAR)3g Derived from Global Inventory Modeling and Mapping Studies (GIMMS) Normalized Difference Vegetation Index (NDVI3g) for the Period 1981 to 2011. *Remote Sens.* **2013**, *5*, 927. [CrossRef]
20. Tucker, C.J. Red and photographic infrared linear combinations for monitoring vegetation. *Remote Sens. Environ.* **1979**, *8*, 127–150. [CrossRef]
21. Lange, M.; Dechant, B.; Rebmann, C.; Vohland, M.; Cuntz, M.; Doktor, D. Validating MODIS and Sentinel-2 NDVI Products at a Temperate Deciduous Forest Site Using Two Independent Ground-Based Sensors. *Sensors* **2017**, *17*, 1855. [CrossRef]
22. Boschetti, M.; Nutini, F.; Manfron, G.; Brivio, P.A.; Nelson, A. Comparative analysis of normalised difference spectral indices derived from MODIS for detecting surface water in flooded rice cropping systems. *PLoS ONE* **2014**, *9*, e88741. [CrossRef] [PubMed]

23. Lu, J.; Ehsani, R.; Shi, Y.; Abdulridha, J.; de Castro, A.I.; Xu, Y. Field detection of anthracnose crown rot in strawberry using spectroscopy technology. *Comput. Electron. Agric.* **2017**, *135*, 289–299. [CrossRef]
24. Manjunath, K.R.; Kumar, A.; Meenakshi, M.; Renu, R.; Uniyal, S.K.; Singh, R.D.; Ahuja, P.S.; Ray, S.S.; Panigrahy, S. Developing Spectral Library of Major Plant Species of Western Himalayas Using Ground Observations. *J. Indian Soc. Remote Sens.* **2013**, *42*, 201–216. [CrossRef]